Video: https://youtu.be/oeuBp__kTSs

A Novel Passive Mechanism for Flying Robots to Perch onto Surfaces

HaoTse Hsiao[1], Feiyu Wu[1], Jiefeng Sun[1], and Jianguo Zhao[1]

***Abstract*— Perching onto objects can allow flying robots to stay at a desired height at low or no cost of energy. This paper presents a novel passive mechanism for aerial perching onto smooth surfaces. This mechanism is made from a bistable mechanism and a soft suction cup. Different from existing designs, it can be easily attached onto and detached from a surface, but it can also hold a large weight when attached to a surface. Further, the mechanism can still work when the suction cup is not precisely aligned with the surface, alleviating the requirement for precise motion control of flying robots. The attachment and detachment are facilitated by the bistable mechanism, while the strong holding is enabled by a locking mechanism that can disable the bistable mechanism. We conduct experiments to characterize the required forces for successful attachments and detachments. We also equip the perching mechanism onto a quadcopter to demonstrate it can be successfully used for perching onto smooth surfaces (e.g., glass).**

I. INTRODUCTION

Flying robots have been recently widely used for various applications, such as 3D mapping, environmental monitoring, disaster relief, precision agriculture, etc [1]. But most existing flying robots, especially quadcopters, cannot stay airborne for a long time because of their limited power supply. In this case, it's better that they can perch/land on objects to save energy while maintaining a desired height for specific applications (e.g., long-duration monitoring tasks) [2], [3]. Among all the objects that a flying robot can land onto, smooth surfaces represent an important category. Being able to perch onto smooth surfaces will greatly enhance flying robots' capability. For instance, they can perch onto the windows of high-rise buildings to perform inspections after a storm. They can also safely land onto a ship deck at sea that may be subject to unpredictable waves [4]. They may also be used to land onto a moving vehicle that may move on an uneven terrain [5].

Nevertheless, the landing/perching process is nontrivial as it involves a complicated perception, planning, and control process. In order to successfully perch onto a surface, the robot needs to rely on sensors (e.g., camera) to detect the surface, estimate the surface's orientation, plan a trajectory, and then follow the trajectory [6], [7]. It also requires a mechanical mechanism that can attach the robot to the surface. Recently, it has been suggested that a properly designed mechanism can be leveraged to enable physical intelligence [8] that can alleviate the requirement for planning and control [9], [10].

*This work is partially supported by National Science Foundation under grants IIS-1815476.

[1]All authors are with the Department of Mechanical Engineering at Colorado State University, Fort Collins, CO, 80523, USA

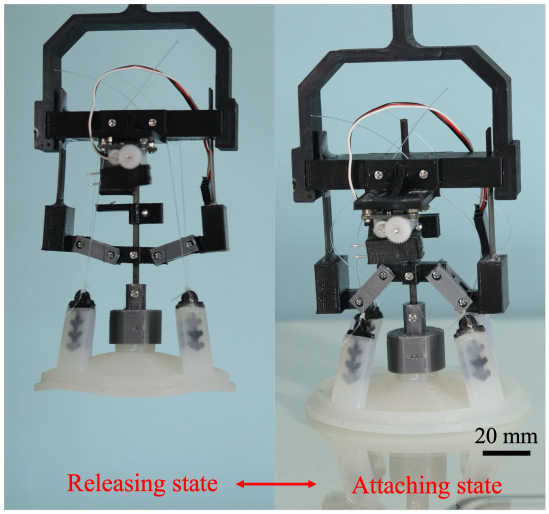

Fig. 1: The prototype of the passive mechanism with its two stable states.

In recent years, researchers have developed various mechanisms for perching onto surfaces based on dry adhesives, electrostatic forces, suction cups, and other methods. For dry adhesives, a flying robot is equipped with several pads with dry adhesives attached. When the robot contacts a surface, the dry adhesive can ensure the robot perch onto the surface [7], [11], [12]. For electrostatic forces, a flying robot has pads that can generate electrostatic forces between the pad and the surface when a high voltage is applied [13], [14]. For suction cups, miniature vacuum pumps are generally used to generate a strong attachment between the robot and the surface [15]–[17], but there also exist passive ones that rely on the impact force [18]. Besides the three main methods, there are other methods such as reverse thrust [19], flip and flap [20], etc.

In this paper, we present the design, development, and experimentation of a passive perching mechanism for flying robots to perch onto smooth surfaces. The mechanism is based on a bistable mechanism and a customized suction cup (Fig. 1). Initially, the suction cup is pulled from the edges by cables attached to the bistable mechanism, enabling easy attachment onto a surface upon contact. After attachment, we can lock the bistable mechanism to generate a strong attachment force that can hold the flying robot. To detach from the surface, we unlock the bistable mechanism, after which a small force can switch the state of the bistable mechanism to allow the cables to pull the suction cup's edges to easily detach from the surface.

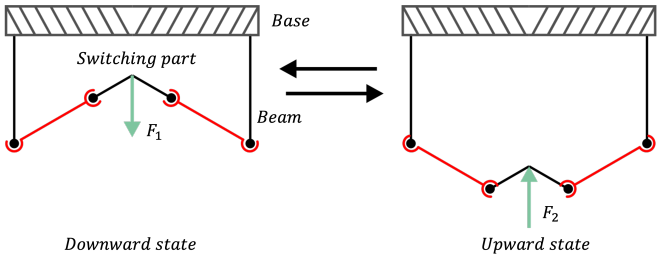

Fig. 2: Diagram of the bistable mechanism with two stable states. Left: the top state shows the switching part is at the top. Right: the bottom state shows the switching part is at the bottom. The bistable mechanism can switch between these two states. When a downward force F_1 is applied, the top state will switch to the bottom state. On the contrary, when an upward force F_2 is applied, the bottom state will switch back to the top state.

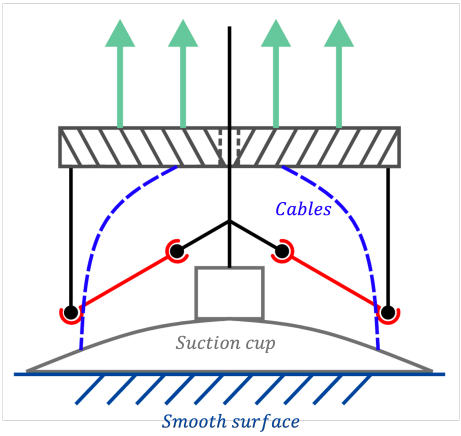

Fig. 3: Diagram of the bistable mechanism integrated with a suction cup.

Our passive perching mechanism has the following advantages compared with existing perching mechanisms based on suction cups. First, it is passive without using vacuum pumps, a heavy part that will decrease a flying robot's payload capability. Attaching to a surface is realized by using the impact force between the mechanism and the surface, while detaching from the surface is accomplished by the thrust force of the flying robot. Second, it can hold a large weight with the locking mechanism, making it suitable for heavy flying robots. Our experimental results show that the passive mechanism, with a mass of 40 g, can hold a quadcopter with a total weight of 601 g. Third, the mechanism can still work when the cup is not fully aligned with the surface, alleviating the requirement for precisely controlling the perching orientation.

The rest of this paper is organized as follows. In section II, we explain the working principle of the proposed perching mechanism. In section III, we discuss the design and fabrication of the mechanism. In section IV, we present the experimental results. In section V, we conclude the paper and discuss future works.

II. WORKING PRINCIPLE

In this section, we introduce the working principle of our mechanism for surface perching. The mechanism includes three main parts: a bistable mechanism, a customized soft suction cup, and a locking mechanism.

The bistable mechanism has two stable states (top and bottom) as shown in Fig. 2. When a downward force F_1 applies on the switching part at the top state of the bistable mechanism (left in Fig. 2), the beams are bent out, and the mechanism switches to the bottom state (right in Fig. 2). On the other hand, when an upward force F_2 is applied on the switching part at the bottom state of the bistable mechanism, it changes back to the top state. The detailed working principle can be found in our previous work [10].

The soft suction cup can attach onto a flat and smooth surface such as the surfaces of glass, metal, or ground materials. After it attaches to a surface, it can withstand a large pulling force applied at the center to remain in the attached state. However, we can easily detach the cup by pulling the edges of the cup. To facilitate the attachment and detachment of the suction cup from a surface, we integrate the suction cup with the bistable mechanism. To maintain the attached state, we use a locking mechanism. In the following, we introduce the integration of the bistable mechanism with the suction cup, and the whole mechanism.

A. Bistable Mechanism with a Suction Cup

The bistable mechanism can be integrated with the soft cup to facilitate the attachment and detachment from a surface. As shown in Fig. 3, we attach the cup's top part to the switching part of the bistable mechanism. We also use cables to connect the cup's edges to the base of the bistable mechanism. By properly adjusting the length of the cables, we can ensure that the edges of the cup will bend upward when the bistable mechanism is at the bottom stable state (bottom left of Fig. 4). Such bending will facilitate attachment to the surface since the cup's center part will contact the surface first and then the edges, ensuring a strong attachment. It will also reduce the requirement for a precise alignment between the cup and the surface. The cables can also facilitate the detachment. If we pull the base of the bistable mechanism upward, the cables will drag the edges to let the cup easily detach from the surface.

B. Working Principle of the Whole Mechanism

After integrating the bistable mechanism with the suction cup, we further add a locking mechanism to ensure the cup can remain the attachment when needed. With the whole mechanism, we explain four main states during a cycle of motion with a simplified sketch (Fig. 4). To illustrate, consider the case that the whole mechanism is installed on the bottom of a quadcopter with an initial releasing state S_r. Note that the mechanism can also be placed on the top or side to perch onto the bottom of a horizontal surface or a vertical surface. During a cycle of motion, the mechanism can undergo the following states: an initial releasing state S_r,

an attached state S_a, a locking state S_l, and an intermediate state S_i. In the following, we discuss the transitions between these states.

Process P_{ra} (from S_r to S_a): When the mechanism is at the initial state S_r, the suction cup cannot form a close enclosure to suck on the surface because its edges are pulled by cables from the base. When the quadcopter lands on a surface, the cup will contact the surface and the downward force from the quadcopter's weight will generate an impact force to push the bistable mechanism transit to the opposite state. Meanwhile, the cables will loosen to allow the cup's edges to contact the surface. In this case, the cup can create the suction force to attach onto the surface, and the mechanism is at the attachment state S_a.

Process P_{al} (between S_a and S_l): When the mechanism attaches to the surface, we use a locking mechanism to ensure it remains attached (state S_l), and we can also unlock the mechanism to make it return to state S_a. To do this, we attach a rod to the switching part of the bistable mechanism The rod can move vertically up and down along with the switching part through a hole at the base. To lock the whole mechanism, we can disable the bistable mechanism by blocking the relative displacement between the base and rod. In this case, the cables will remain loose and cannot apply force to the edge of the suction cup. Instead, all the force is applied at the cup's top center, allowing the suction cup to stay in place even with a very large upward force. To unlock the mechanism, we can enable the bistable mechanism to allow relative displacement between the base and the rod. In this case, the system can return back to state S_a.

Process P_{ai} (from S_a to S_i): At state S_a, when the quadcopter flies upward, generating an upward force that will pull the whole mechanism to an intermediate state S_i. During this process, the suction cup is still attached onto the surface because all upward force is applied to the center of the suction cup. Meanwhile, the cables are gradually tensioned but not fully tensioned to pull the cup's edges.

Process P_{ir} (from S_i to S_r): After the mechanism crosses state S_i, the state will rapidly transit to the initial state S_r because of the bistable mechanism. During this process, the cables start to pull the cup's edges, and the air leaks into the cup to release the cup from the surface. Then, the quadcopter can fly away from the surface.

The whole process can form a loop to allow the passive mechanism to successfully accomplish perching/landing onto a surface. Because the edges are pulled by the cables at the initial state S_i, the mechanism can still work when the cup is not fully aligned with the surface. In other words, we will not need to control the perching orientation very precisely.

III. DESIGN AND FABRICATION

In this section, we elaborate the design and fabrication of the three main parts: the bistable mechanism, the suction cup, and the locker, which are individually shown in Fig. 5a-c. A whole assembly of all the three mechanisms without the cables is shown in Figure 5d.

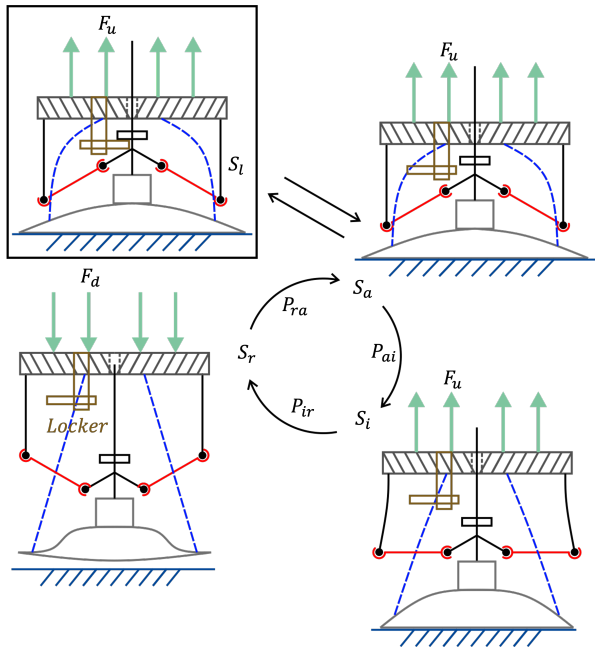

Fig. 4: Illustrations for the perching mechanism's working principle. The bottom left sketch shows the initial releasing state S_r. When a downward for F_d is applied, S_r will transit to attaching state S_a (top right sketch). If the locker (brown color sketch) locks, the mechanism will transit to locking state S_l (top left sketch), and it can also go back to S_a when unlocked. When at state S_a, an upward force will make it first transit to the intermediate state S_i (bottom right), which will rapidly switch back to the original state S_r.

The bistable mechanism shown in Fig. 5a includes one switch part, two beams on both sides, two beam heads at the beam's end, two links to connect the switch part and beam heads, one rigid base with a hole for linear guide rod, and linear guide rod to guarantee vertical displacement. All of them except the beams are 3D printed. The two bendable beams are flat carbon fiber (Width×Thickness: 7.9 × 0.8 mm, CF312032048, Goodwinds Composites LLC). We can also manually adjust the effective length of the carbon fiber using screws at the base.

The suction cup is connected to the bistable mechanism's linear guide rod through a 3D printed cup head. Four 3D printed pullers are embedded inside the cup's edges as shown in Fig. 5b. The pullers are used for connecting cables to the base to enhance the edges' strength. Detailed fabrication procedures of the suction cup will be introduced later.

The locker part can lock the bistable mechanism to block the relative displacement between the base and linear guide rod. Figure 5c shows the locker part, including a rod latch, a motor base, a latch support, and a locker latch. The motor base hosts a linear servo motor (GS1502, Flash Hobby) on the base of the bistable mechanism. The rod latch is fixed to the linear guide rod. When the rod latch is above the locker latch, the servo motor will actuate the locker latch to move along the red dash arrow to prevent the downward

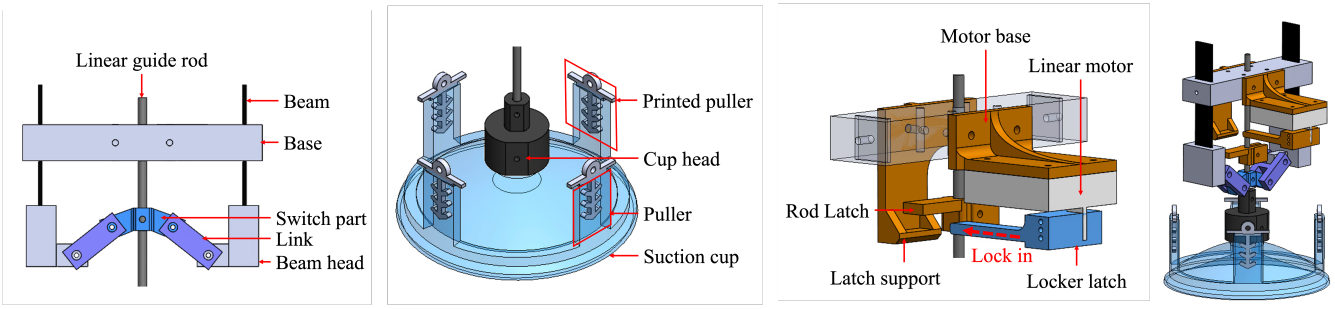

(a) (b) (c) (d)

Fig. 5: The structure diagrams of (a) the bistable mechanism, (b) the suction cup, (c) the locker, and (d) the assembly of all of them.

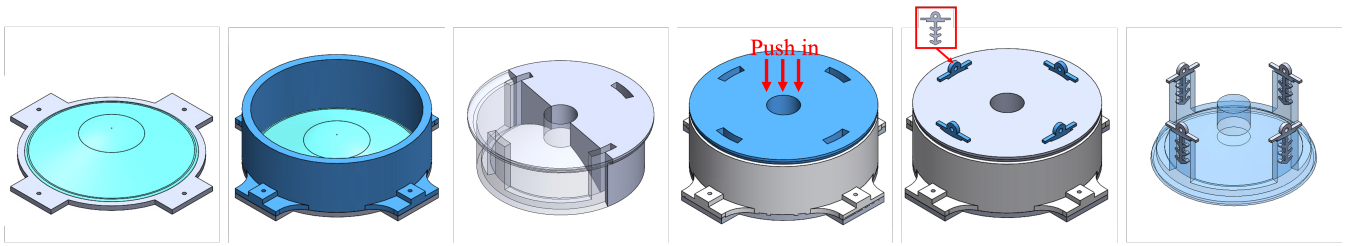

(a) (b) (c) (d) (e) (f)

Fig. 6: Fabrication process for the soft suction cup. (a) Coating a thin layer of XTC-3D (light blue color) on the bottom mold to fabricate a smooth surface. (b) Combining the wall mold with bottom mold, then the dragon skin is filled into the mold until half level. (c) The cross-section view of top mold. (d) The top mold is slowly pushed into the combined mold. (e) The pullers (top left sketch) is placed in the four holes, additional dragon skin is poured to fill into the mold fully, and the mold is placed into the vacuum to remove the bubbles inside the dragon skin 30. (f) The suction cup can be demolded after four hours curing.

movement of the rod latch. In this case, the whole mechanism is locked since the bistable mechanism cannot switch from the attaching state to the next state.

The suction cup part is fabricated using a molding approach with silicone rubber (Dragon Skin 30, Smooth-On Inc.). The final mold is an assembly of three 3D printed molds: the bottom mold, the wall mold, and the top mold as shown in Fig. 6. The fabrication procedure is shown in Fig. 6. First, the upper surface of the bottom mold is painted with a layer of XTC-3D (Smooth-On Inc.) to form a smooth surface (Fig. 6a) that will ensure a good vacuum seal of the suction cup. Then, the wall mold is screwed on the bottom mold, and the dragon skin 30 is filled into it (Fig. 6b). The top mold can be placed inside the wall mold and a cross-section view is shown in 6c. After filling some dragon skin 30 to the half level of volume of the combined mold, the top mold is assembled. During the process, we slowly push the top mold to avoid introducing more air or bubbles (Fig. 6d). Then, the whole mold with filled dragon skin 30 is put into a vacuum to remove the air bubbles. Finally, the printed pullers with some fin features are plugged into the hole of the top mold to increase the strength of the pulling parts (Fig. 6e). Finally, we demold the cup from the mold after curing for four hours (Fig. 6f).

IV. EXPERIMENTS AND RESULTS

In this section, we experimentally characterize the passive mechanism and conduct a perching/landing experiment. For the passive mechanism, we mainly obtain the force-displacement relationship for different processes to verify the design of the passive mechanism in Sec. II-B and Fig. 4. Note that all force and displacement data during experiments are measured by a motorized test stand (ESM303, Mark-10). For showing every force-displacement relationship experiment, we use the means and shade errors to represent 3 tests.

A. Maintenance Force of S_r

When the passive mechanism is at S_r, we need to ensure the bistable mechanism stays at the bottom stable state. This means the tension force in the cable F_s should be small enough to prevent the bistable mechanism from switching the state. In other words, F_s should be smaller than the maximum of the switching force F_b for the bistable mechanism to stay in state S_r. Therefore, we set up the experiments to test F_s and F_b.

First, we experimentally obtain how F_s will change with respect to the cup edge's vertical displacement. For this experiment, we fix the cup's center and use the test stand to pull the cup's edge vertical up and record the force and displacement. The result is shown in Fig. 7, where the

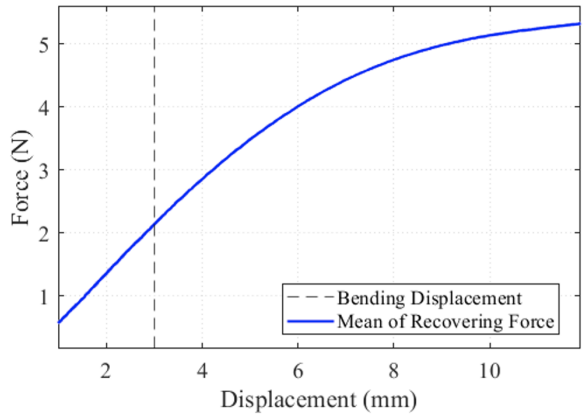

Fig. 7: The force-displacement relationship of the suction cup when the cables pull the cup's edge from 0 to 12 mm. The black dash line represents the force (2.1 N) required to pull the cup for 3 mm.

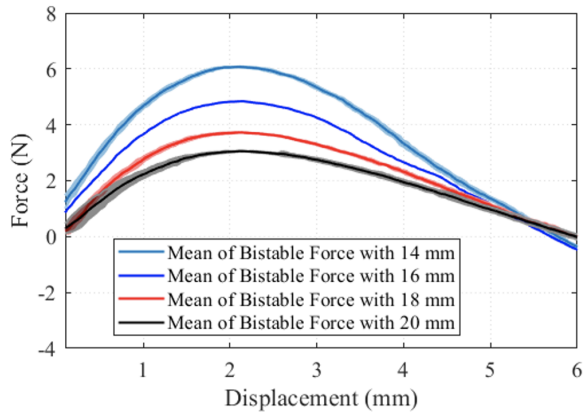

Fig. 8: The force-displacement relationship of bistable mechanism. The force F_b first increases and then decreases with respect to the displacement of the switch part for different effective beam lengths (14, 16, 18, and 20 mm).

force increases with the vertical displacement from 0 to 12 mm. With the result, we choose to make the initial vertical displacement of the cup's edge for S_r to be 3 mm. With this value, the maximum of F_s is about 2.1 N (black dash line in Fig. 7) to ensure the whole mechanism can stay in state S_r based on the maximum switching force for the bistable mechanism in the following paragraph. Note that the initial displacement of the cup's edge can be adjusted by changing the length of cables.

Second, the force F_b applying to the bistable mechanism to switch the state is related to the bending stiffness of the beam, which is further determined by the effective length of the beam. We directly measured the relationship between the effective length of beams and F_b by holding the base and using the test stand to push the switch part. Fig. 8 shows how F_b changes with respect to the displacement of the switch part. To keep S_r, the effective length of beams should be adjusted to make sure the maximum value of F_b:

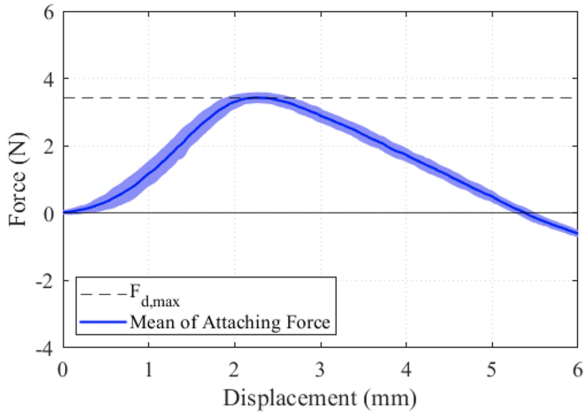

Fig. 9: The force-displacement relationship of the passive mechanism during the process P_{ra}. The force F_d will first increase and then decrease. The black dash line is $F_{d,max}$ to transit the state from S_r to S_a.

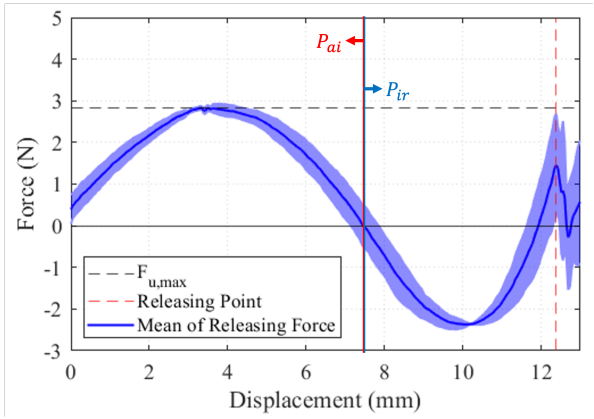

Fig. 10: The force-displacement relationship of the passive mechanism during process P_{ai} and P_{ir}. The force F_u will first increase, decrease to the opposite direction, and then increase again. P_{ai} is before the red-blue line and P_{ir} is after the red-blue line. The black dash line is $F_{d,max}$ to transit the state from S_a to S_i. The red dash line is the releasing point to achieve S_r.

$F_{b,max} > F_s$. For example, if the maximum of F_s is about 2.1 N (corresponding to 3 mm vertical displacement of the cup's edge), the effective length of the beams is required to be less than 20 mm as shown in Fig. 8.

B. Attaching Force Experiment

The attaching force is the maximum value of the downward force $F_{d,max}$ to let S_r transit to S_a during P_ra. To obtain this force, we integrate the bistable mechanism and the soft cup. During the experiment, we hold the base, gradually push the cup onto a smooth glass using the test stand. The force-displacement relationship during the process is shown in Fig. 9. When F_d is applied on the base, once F_d is larger than $F_{d,max}$ which is 3.43 N with an effective beam length of 20 mm, the suction cup at S_r will transit to S_a. The mass of the quadcopter in our lab is 601 g (5.89 N) with the

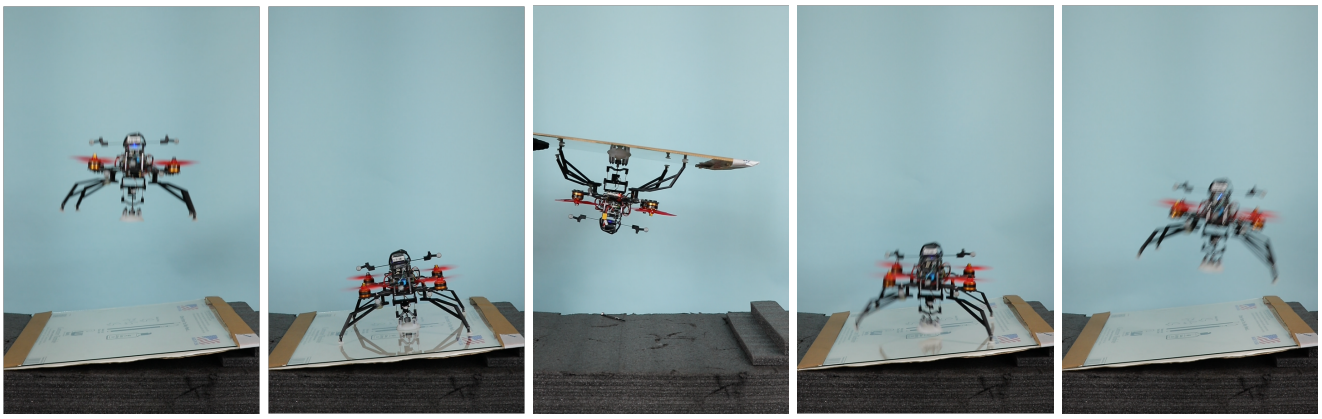

(a) (b) (c) (d) (e)

Fig. 11: Perching experiment. (a) The passive mechanism can keep S_r during the flight. (b) The quadcopter with the passive mechanism can land on a glass plate with 6 degrees tilting angle. (c) Once the locker is locked, the passive mechanism cannot transit to S_i and the quadcopter keeps attaching on the glass. even though the glass is flipped upside down. (d) While the mechanism is unlocked, the quadcopter can fly up and the passive mechanism transit to S_r. (e) Finally, the quadcopter can fly away.

passive mechanism, which is greater than $F_{d,max} = 3.43$ N. Therefore, the quadcopter can passively attach to land on smooth and flat surfaces.

C. Releasing Force Experiment

An upward releasing force F_u should be applied to switch the state from S_a to S_i, after which the state will be automatically transit to the initial state S_r. We also experimentally obtain the required releasing force for the developed mechanism. For this experiment, we first attach the whole mechanism onto a piece of glass, and then hold the base, gradually pull the mechanism from the glass using the test stand. Fig. 10 shows the force-displacement relationship during P_{ai} and P_{ir}. In Fig. 10, the vertical solid line separates the whole process into P_{ai} and P_{ir}. During P_{ai} which is before the red-blue solid line, the cables are not pulling the cup's edges. If F_u crosses the maximum of the upward force $F_{u,max}$ with 2.83 N with an effective length of the beams 20 mm, the process will cross S_i and keep going to P_{ir} which is after the red-blue solid line. During P_{ir}, the cables start pulling the cup's edges. After the vertical displacement is at 12.38 mm (red dash line), the cup separates from the surface, and the state completes the transition to S_r.

D. Aerial Perching Experiment

We conduct the aerial perching experiment to verify the working principle of the passive mechanism. The mechanism is fixed onto the bottom of a customized quadcopter developed in our lab. The total weight of the quadcopter is 601 g with the mechanism. Fig. 11 shows the aerial perching experiment results. Figure 11a shows the quadcopter carries the passive mechanism in S_r state while it is hovering. The initial vertical displacement of the cup's edge by the cables is 3 mm. Then, the quadcopter lands on the smooth glass with a tilting angle of 6 degrees, and the passive mechanism transits the states from S_r to S_a (Fig. 11b). After that, the locker is locked in and the state transits to S_l. Consequently, the quadcopter with the locked mechanism can remain on the glass even though the glass plate is shaking or upside down (Fig. 11c). Finally, when the mechanism is unlocked, the quadcopter at S_a can fly away and the state will transit to S_r (Fig. 11d and Fig. 11e).

Since it is difficult to fly the quadcopter up from a surface with a large tilted angle due to the large recovery moment and our confined flying space, we conduct several landing experiments by manually dropping the quadcopter to surfaces with different angles to demonstrate the robustness of the perching mechanism. Additional experiments are shown in the supplementary video.

V. CONCLUSIONS

In this work, we presented a novel passive mechanism that can be equipped on a flying robot to allow for its perching. The mechanism can attach onto and detach from a smooth surface automatically. The softness of the suction cup allows the mechanism to increase the robustness of the attaching process for surfaces with different tilting angles. We introduced the working principle of the mechanism and its fabrication process. Experiments are conducted to characterize the mechanism. The final demonstration shows that the mechanism installed on the bottom of a quadcopter allows it to perch on surfaces with different tilting angles. When the locking mechanism is locked, the mechanism can reliably remain attached to the surface. Once unlocked, the mechanism can detach from the surfaces when the quadcopter takes off. With proper planning and control, we envision the mechanism can be implemented on a variety of flying robots to allow them to attach onto smooth fixed surfaces such as ceilings, vertical walls, or moving surfaces of vehicles, ships, or even other flying robots.

REFERENCES

[1] D. Floreano and R. J. Wood, "Science, technology and the future of small autonomous drones," *Nature*, vol. 521, no. 7553, pp. 460–466, 2015.

[2] K. Hang, X. Lyu, H. Song, J. A. Stork, A. M. Dollar, D. Kragic, and F. Zhang, "Perching and resting—a paradigm for uav maneuvering with modularized landing gears," *Science Robotics*, vol. 4, no. 28, p. eaau6637, 2019.

[3] W. Roderick, M. Cutkosky, and D. Lentink, "Bird-inspired dynamic grasping and perching in arboreal environments," *Science Robotics*, vol. 6, no. 61, p. eabj7562, 2021.

[4] J. L. Sanchez-Lopez, J. Pestana, S. Saripalli, and P. Campoy, "An approach toward visual autonomous ship board landing of a vtol uav," *Journal of Intelligent & Robotic Systems*, vol. 74, no. 1, pp. 113–127, 2014.

[5] T. Baca, P. Stepan, V. Spurny, D. Hert, R. Penicka, M. Saska, J. Thomas, G. Loianno, and V. Kumar, "Autonomous landing on a moving vehicle with an unmanned aerial vehicle," *Journal of Field Robotics*, vol. 36, no. 5, pp. 874–891, 2019.

[6] H. Zhang, B. Cheng, and J. Zhao, "Optimal trajectory generation for time-to-contact based aerial robotic perching," *Bioinspiration & biomimetics*, vol. 14, no. 1, p. 016008, 2018.

[7] J. Thomas, M. Pope, G. Loianno, E. W. Hawkes, M. A. Estrada, H. Jiang, M. R. Cutkosky, and V. Kumar, "Aggressive flight with quadrotors for perching on inclined surfaces," *Journal of Mechanisms and Robotics*, vol. 8, no. 5, 2016.

[8] M. Sitti, "Physical intelligence as a new paradigm," *Extreme Mechanics Letters*, vol. 46, p. 101340, 2021.

[9] H. Zhang, J. Sun, and J. Zhao, "Compliant bistable gripper for aerial perching and grasping," in *2019 International Conference on Robotics and Automation (ICRA)*. IEEE, 2019, pp. 1248–1253.

[10] H. Zhang, E. Lerner, B. Cheng, and J. Zhao, "Compliant bistable grippers enable passive perching for micro aerial vehicles," *IEEE/ASME Transactions on Mechatronics*, 2020.

[11] L. Daler, A. Klaptocz, A. Briod, M. Sitti, and D. Floreano, "A perching mechanism for flying robots using a fibre-based adhesive," in *2013 IEEE International Conference on Robotics and Automation*. IEEE, 2013, pp. 4433–4438.

[12] A. Kalantari, K. Mahajan, D. Ruffatto, and M. Spenko, "Autonomous perching and take-off on vertical walls for a quadrotor micro air vehicle," in *2015 IEEE International Conference on Robotics and Automation (ICRA)*. IEEE, 2015, pp. 4669–4674.

[13] M. Graule, P. Chirarattananon, S. Fuller, N. Jafferis, K. Ma, M. Spenko, R. Kornbluh, and R. Wood, "Perching and takeoff of a robotic insect on overhangs using switchable electrostatic adhesion," *Science*, vol. 352, no. 6288, pp. 978–982, 2016.

[14] S. Park, D. S. Drew, S. Follmer, and J. Rivas-Davila, "Lightweight high voltage generator for untethered electroadhesive perching of micro air vehicles," *IEEE Robotics and Automation Letters*, vol. 5, no. 3, pp. 4485–4492, 2020.

[15] H. Tsukagoshi, M. Watanabe, T. Hamada, D. Ashlih, and R. Iizuka, "Aerial manipulator with perching and door-opening capability," in *2015 IEEE International Conference on Robotics and Automation (ICRA)*. IEEE, 2015, pp. 4663–4668.

[16] C. C. Kessens, J. Thomas, J. P. Desai, and V. Kumar, "Versatile aerial grasping using self-sealing suction," in *2016 IEEE international conference on robotics and automation (ICRA)*. IEEE, 2016, pp. 3249–3254.

[17] S. Liu, W. Dong, Z. Ma, and X. Sheng, "Adaptive aerial grasping and perching with dual elasticity combined suction cup," *IEEE Robotics and Automation Letters*, vol. 5, no. 3, pp. 4766–4773, 2020.

[18] H. W. Wopereis, T. Van Der Molen, T. Post, S. Stramigioli, and M. Fumagalli, "Mechanism for perching on smooth surfaces using aerial impacts," in *2016 IEEE international symposium on safety, security, and rescue robotics (SSRR)*. IEEE, 2016, pp. 154–159.

[19] J. Bass and A. L. Desbiens, "Improving multirotor landing performance on inclined surfaces using reverse thrust," *IEEE Robotics and Automation Letters*, vol. 5, no. 4, pp. 5850–5857, 2020.

[20] Z. Huang, S. Li, J. Jiang, Y. Wu, L. Yang, and Y. Zhang, "Biomimetic flip-and-flap strategy of flying objects for perching on inclined surfaces," *IEEE Robotics and Automation Letters*, vol. 6, no. 3, pp. 5199–5206, 2021.